

# CRACK INITIATION MODELING IN BIAXIAL LOW CYCLE FATIGUE AND SIMULATION OF GRAIN GEOMETRY EFFECT ON FATIGUE DAMAGE

T. HOSHIDE

Department of Energy Conversion Science, Kyoto University, Japan

## ABSTRACT

In biaxial low cycle fatigue, especially, spatial distribution of initiated cracks may affect the subsequent growth of a dominant crack, which sometimes depends on stress multiaxiality as well as material microstructure. In this work, the crack initiation in biaxial stress state was first modeled as the slip band formation in an individual grain constituting a polycrystalline metal. In modeled grains, normal directions of slip planes and slip directions on respective planes were independently given at random. Since stress states in individual grains were supposed to be different from the bulk one, stresses in each grain were also randomly given under some restrictions. A slip-band crack was presumed to be initiated along the given slip direction on the specified slip plane when the resolved shear stress in the slip direction exceeded a critical shear stress. The crack initiation life was also calculated using a dislocation pile-up model. By simulations using the proposed model, the directional distributions and initiation lives of initiated cracks were obtained for mixed modes. Effects of the size and aspect ratio of grain on the directional distribution of cracks were investigated. It was found that simulated results showed a good agreement with experimental observations.

## 1 INTRODUCTION

Failure life in multiaxial fatigue is dominated by cracking behavior which depends on the material microstructure as well as the stress multiaxiality (e.g., Hua [1], Bannatine [2], Hoshide [3]). In low cycle fatigue, especially, many small cracks are sometimes initiated and the linkage of small cracks is predominant mode of crack growth. Consequently, the spatial distribution of initiated cracks may be important for the subsequent growth of a dominant crack, which yields substantial fatigue damage in such a situation. In polycrystalline metals, there are preferential sites of crack initiation according to stress level and material (Boettner [4], Laird [5], Brown [6]). Since the crack nucleation is considered to be a consequence of the crystallographic sliding in a grain, an analysis of slip band formation in a grain is beneficial in the evaluation of fatigue damage.

In this work, crack initiation under biaxial fatigue was modeled as the slip band formation in an individual grain constituting a polycrystalline metals. Simulations using the proposed model were conducted to investigate space-time distribution of initiated cracks for various values of biaxiality. Simulated directions of initiated cracks under biaxial stress states were compared with experimental results observed in biaxial fatigue using a pure copper and ( $\alpha+\beta$ ) Ti alloy, which have different microstructures, and the applicability of the proposed model was discussed.

## 2 MODELING OF CRACK INITIATION

### 2.1 Coordinates and stresses associated with slip systems

A Cartesian  $x$ - $y$ - $z$  coordinate, in which the  $y$  and  $z$  axes are respectively parallel to the specimen axis and the normal direction of the specimen surface, is introduced (see Fig. 1). Consider a slip plane in one grain on the specimen surface. Another orthogonal  $\xi$ - $\eta$ - $\zeta$  coordinate is constituted by the normal direction  $\xi$  of the slip plane and the slip direction  $\eta$  on the slip plane.

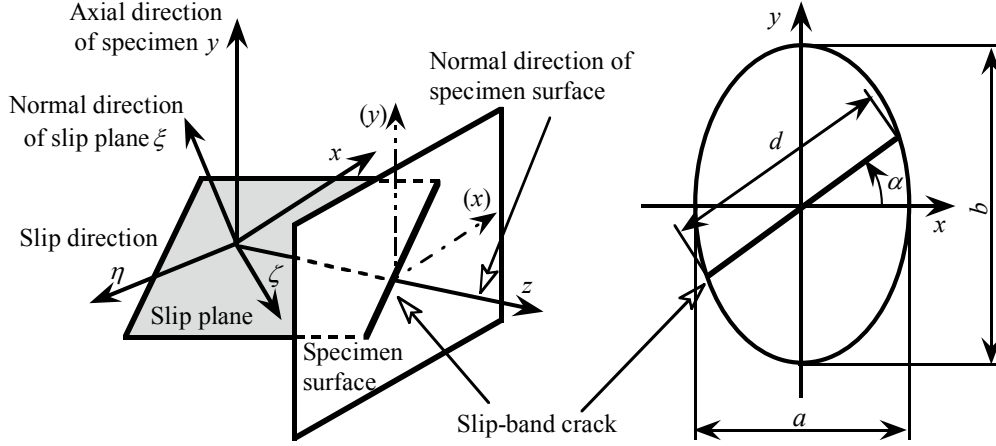


Figure 1: Relation between specimen surface and slip plane, and direction of slip-band crack.

Stress tensors  $[\sigma_{xyz}]$  and  $[\sigma_{\xi\eta\zeta}]$  are respectively defined in  $x$ - $y$ - $z$  and  $\xi$ - $\eta$ - $\zeta$  coordinates, and directional cosine tensor  $[l]$  is determined between the two coordinates; i.e.

$$[\sigma_{xyz}] = \begin{bmatrix} \sigma_x & \tau_{xy} & \tau_{zx} \\ \tau_{xy} & \sigma_y & \tau_{yz} \\ \tau_{zx} & \tau_{yz} & \sigma_z \end{bmatrix}, \quad [\sigma_{\xi\eta\zeta}] = \begin{bmatrix} \sigma_\xi & \tau_{\xi\eta} & \tau_{\zeta\xi} \\ \tau_{\xi\eta} & \sigma_\eta & \tau_{\eta\zeta} \\ \tau_{\zeta\xi} & \tau_{\eta\zeta} & \sigma_\zeta \end{bmatrix}, \quad \text{and } [l] = \begin{bmatrix} l_{x\xi} & l_{x\eta} & l_{x\zeta} \\ l_{y\xi} & l_{y\eta} & l_{y\zeta} \\ l_{z\xi} & l_{z\eta} & l_{z\zeta} \end{bmatrix}. \quad (1)$$

The stress  $[\sigma_{\xi\eta\zeta}]$  for the slip system is correlated with an applied stress  $[\sigma_{xyz}]$  as

$$[\sigma_{\xi\eta\zeta}] = [l] [\sigma_{xyz}] [l]^T, \quad (2)$$

where the superscript “T” means the transposed matrix. Considering slip in a surface grain, we may assume the plane stress state, i.e.,  $\sigma_z = \tau_{yz} = \tau_{zx} = 0$ . Under this assumption, two stress parameters are dealt with on the slip plane. The resolved shear stress  $\tau_{\xi\eta}$  in the slip direction is one of the most important factor for the feasibility to slip, and is represented by

$$\tau_{\xi\eta} = \sigma_x l_{x\xi} l_{y\xi} + \sigma_y l_{x\eta} l_{y\eta} + \tau_{xy} (l_{x\xi} l_{y\eta} + l_{x\eta} l_{y\xi}). \quad (3)$$

The normal stress  $\sigma_\xi$  associated with the split resistance between slip planes is expressed as

$$\sigma_\xi = \sigma_x l_{x\xi}^2 + \sigma_y l_{x\eta}^2 + 2\tau_{xy} l_{x\xi} l_{x\eta}. \quad (4)$$

## 2.2 Initiation model of slip-band crack

The slip plane,  $\eta$ - $\zeta$  plane, is expressed in the  $x$ - $y$ - $z$  ordinate as follows.

$$l_{x\xi} x + l_{y\xi} y + l_{z\xi} z = 0 \quad (5)$$

On the specimen surface, the slip-band is presented as  $y = Cx + D$  with  $D = -(l_{z\xi}/l_{y\xi})\delta$ , where  $\delta$  is the distance from the origin of  $x$ - $y$ - $z$  ordinate to the specimen surface in the  $z$  direction. Comparing with Eqn. (5), the coefficient  $C$  is calculated as  $C = -l_{x\xi}/l_{y\xi}$ . The angle  $\alpha$  of slip-band is defined counterclockwise against the  $x$  axis on the specimen surface, and is calculated as

$$\alpha = \arctan(-l_{x\xi}/l_{y\xi}). \quad (6)$$

A crack is assumed to be initiated along the slip band if the following criterion is satisfied.

$$(\tau_{\xi\eta} / \tau_c) \geq 1, \quad (7)$$

where  $\tau_c$  is the critical shear stress to make a slip active. A crack generated along the active slip band is hereafter designated “slip-band crack” or just SBC. It is presumed that the initiation life

$N_i$  of SBC is calculated by using a dislocation pile-up model (Tanaka [7]) as follows.

$$N_i = \frac{2GW_c}{\pi(1-\nu)d_o(\tau_c)^2} \cdot \frac{1}{(d/d_o)(\tau_{\xi\eta}/\tau_c - 1)^2}, \quad (8)$$

where  $G$ ,  $\nu$ ,  $W_c$  and  $d_o$  are respectively the shear elastic modulus, Poisson's ratio, the surface energy and the mean grain size. The parameter  $d$  is a size of grain to be considered in the slip analysis. In the following, the initiation life  $N_i$  is normalized by  $N_o = 2GW_c / [\pi(1-\nu)d_o(\tau_c)^2]$  which consists of only material constants. The normalized life  $\bar{N}_i$  is finally expressed as

$$\bar{N}_i = \frac{1}{(d/d_o)(\tau_{\xi\eta}/\tau_c - 1)^2}. \quad (9)$$

### 2.3 Expression of randomness in crack initiation analysis

Since individual grains actually differ in geometrical shapes and deformation responses in actual polycrystalline materials, a stress state in one grain is supposed to differ from that in another grain. Therefore, it is reasonable to consider that stresses, to which individual grains are subjected, are different from the bulk applied stress. The present model assumes that stresses deviate from the given applied stress, and the stress components  $\sigma_x^{(i)}$ ,  $\sigma_y^{(i)}$  and  $\tau_{xy}^{(i)}$  of the  $i$ -th grain are given by

$$\sigma_x^{(i)} = \sigma_x f_i \text{ with } \sum_{i=1}^n f_i/n = 1, \quad \sigma_y^{(i)} = \sigma_y g_i \text{ with } \sum_{i=1}^n g_i/n = 1, \quad \text{and} \quad \tau_{xy}^{(i)} = \tau_{xy} h_i \text{ with } \sum_{i=1}^n h_i/n = 1 \quad (10)$$

where  $\sigma_x$ ,  $\sigma_y$  and  $\tau_{xy}$  are components of the applied stress, and  $n$  is the number of analyzed grains.

Another randomness to be expected in actual materials is associated with the slip system in distinct grains as constituents of the material under consideration. For each grain with the slip line angle  $\alpha$ , the directional cosines related with the slip system in the grain are randomly given under the restrictions for those cosine parameters with eqn (5), which should be satisfied.

We also have to consider the variation in size of individual grain, so the randomness of grain size is expressed by using another deviation factor  $r_i$ ; i.e., the size of the  $i$ -th grain,  $d^{(i)}$ , is given as

$$d^{(i)} = d_o r_i \quad \text{with} \quad \sum_{i=1}^n r_i/n = 1. \quad (11)$$

Sometimes, a geometric anisotropy is seen in grains stretched by rolling or machining. In this modeling, the shape of such a stretched grain is treated as an ellipse with length  $a$  and  $b$  of minor and major axes respectively. In calculating the initiation life by eqn (9),  $d$  as illustrated in Fig. 1 is used for the length of SBC and the value of  $d$  is given by

$$d = \frac{b}{\sqrt{\Lambda^2 \cos^2 \alpha + \sin^2 \alpha}}, \quad (12)$$

where  $\Lambda = b/a$  is the aspect ratio of a grain and  $\Lambda = 1$  implies an isotropic microstructure.

### 2.4 Introduction of "intensity of slip-band crack"

A new parameter is introduced as "intensity of slip-band crack",  $I_{\text{SBC}}$ , which is defined by

$$I_{\text{SBC}} = (d/d_o) |l_{z\eta}| = (d/d_o) (1 - l_{x\eta}^2 - l_{y\eta}^2)^{1/2}. \quad (13)$$

The parameter  $I_{\text{SBC}}$  may correspond to a relative area of the slip plane which appears on the specimen surface. A larger value of  $I_{\text{SBC}}$  implies a larger slip in the grain under consideration, and so the parameter  $I_{\text{SBC}}$  is expected to represent the possibility of crack initiation.

## 3 SIMULATION PROCEDURES

By preparatory simulations, it is found that the effect of the grain size variation is not so significant and the normal stress  $\sigma_z$  doesn't affect the simulated result. Therefore, the effect of

grain shape, especially the aspect ratio  $A$ , will be investigated in this work.

The randomness of the stress variation was only dealt with, and the deviation factors,  $f_i$ ,  $g_i$  and  $h_i$ , were randomly given in the range from 0.5 to 1.5.

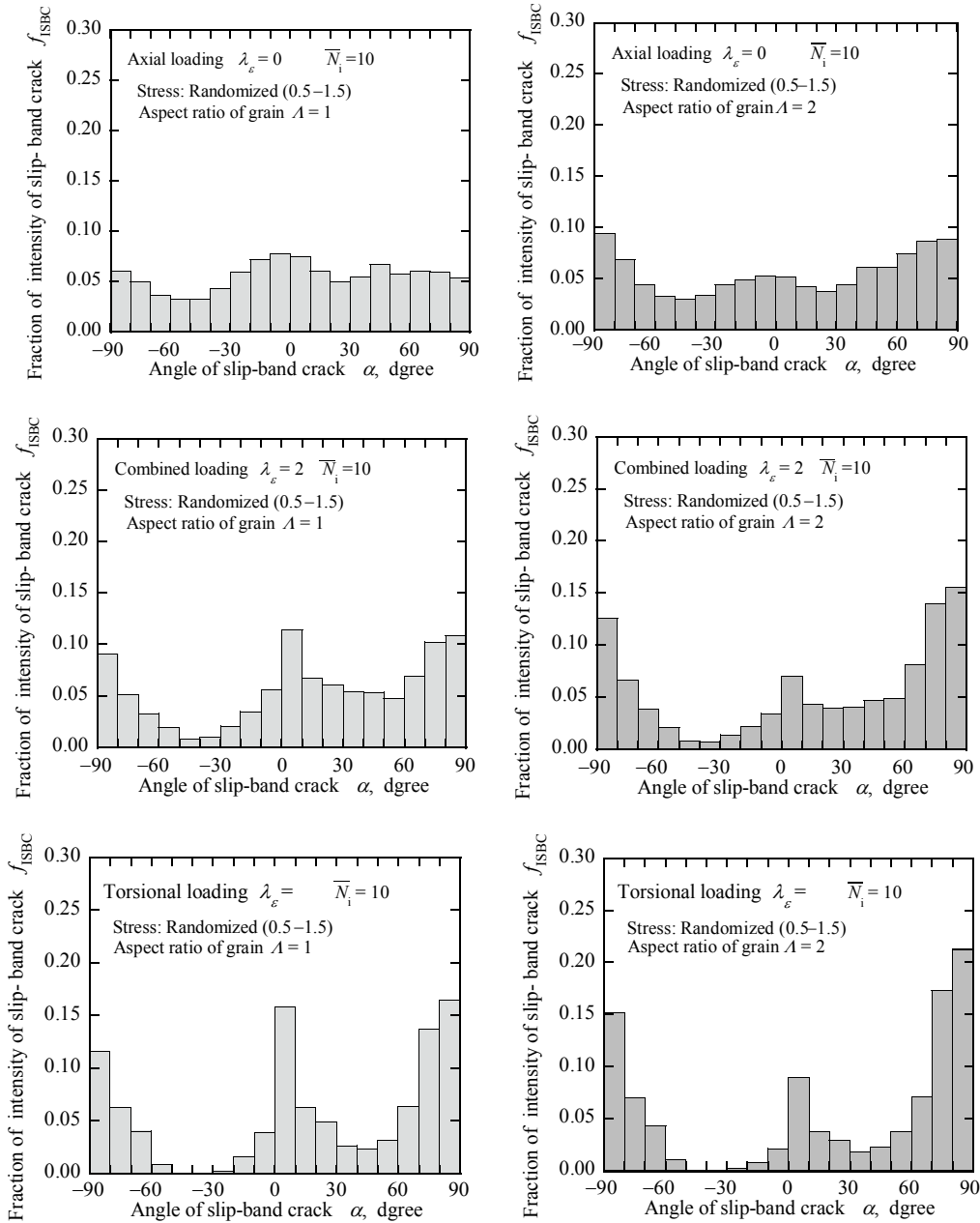


Figure 2: Distribution of slip-band crack orientation obtained by simulation for  $A = 1$ .

Figure 3: Distribution of slip-band crack orientation obtained by simulation for  $A = 2$ .

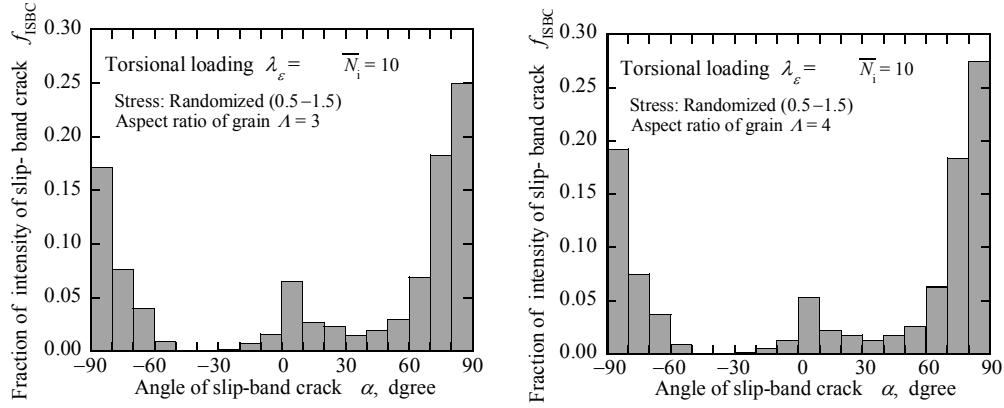


Figure 4: Effect of grain aspect ratio on angle distribution of slip-band crack in torsion.

For a given angle  $\alpha$  of SBC, the directional cosine components of  $[l]$  were randomized under the restricted conditions of cosine parameters. For these randomizations, the resolved shear stress  $\tau_{\xi\eta}$  of eqn (3) can be calculated and also the initiation life is determined by eqn (9) when  $\tau_{\xi\eta} > \tau_c$ . A different distribution of SBC angle  $\alpha$  may be obtained according to the number of cycles. The intensity of SBC,  $I_{SBC}$ , was compared with the experimental observation through a histogram of a cumulative  $I_{SBC}$ -value for  $\alpha$ . 8,100 combinations of ninety normal directions of slip plane and ninety slip directions on the respective slip planes were randomly given for a specified angle  $\alpha$  in the range from  $-90^\circ$  to  $+90^\circ$ , by considering the symmetry of the angle  $\alpha$  with respect to the  $x$  axis.

## 4 SIMULATED RESULTS AND DISCUSSIONS

### 4.1 Summary of experimental observations

Experimental works (Inoue [8], Hoshide [9]) have been carried out. The fatigue tests were conducted under axial, torsional, and in-phase combined axial-torsional loading modes. The material used in experiments was an oxygen-free pure copper, which has a quasi-isotropic microstructure. This material will be used as a reference material in a sense of isotropy. Another material was an  $(\alpha+\beta)$  Ti alloy, grains of which were stretched in the axial direction (coinciding with its rolling direction). As for the  $(\alpha+\beta)$  Ti alloy, the average aspect ratio of stretched  $\alpha$ -grains, which were preferable sites for crack initiation, was approximately 2.

By the observation of fatigue cracks, the subsequent crack growth was found to be dominated by coalescence of distributed cracks. In the copper, the orientation of the dominant crack at a final stage was nearly perpendicular to the direction of the principal stress in the case of axial and combined modes, but was parallel to the maximum shear stress directions in the case of torsion. In the torsion of the Ti alloy, especially, the main crack grew only in the axial direction.

### 4.2 Simulated results

The experimental observation in the copper with quasi-isotropic microstructure revealed that at early stages of fatigue, around  $N/N_f = 0.2$ , the distribution of SBC has distinct peaks depending on the strain biaxiality as follows;  $-70^\circ < \alpha < +70^\circ$  for  $\lambda_\epsilon = 0$ ,  $\alpha = -10^\circ \sim -20^\circ$  and  $+60^\circ \sim +70^\circ$  for  $\lambda_\epsilon = 2$ , and  $\alpha = 0^\circ$  and  $\pm 90^\circ$  for  $\lambda_\epsilon = \infty$ , respectively. These peaks almost coincide with the angles of the maximum shear directions according to stress states. For each loading mode, Figs 2 and 3 show the simulated distributions with setting  $A = 1$  and  $A = 2$ , respectively, at the normalized

number of cycles  $\bar{N}_1 = 10$ , which is supposed to represent a state in an early stage of fatigue. As for a quasi-isotropic material ( $\lambda \cong 1$ ), it may be concluded that the simulated results approximately present the experimental observation in copper. On the other hand, the peak level around  $\pm 90^\circ$  becomes higher in the distribution for a material with  $\lambda = 2$  like a stretched grain, compared with the case of  $\lambda = 1$ . This trend is found to be more remarkable in torsional mode. Figure 4 shows the angle distribution for larger aspect ratios  $\lambda$ , especially in torsional mode. The distribution of SBC angle shifts toward the side around  $\pm 90^\circ$  for a larger  $\lambda$ . The result almost coincides with the experimental observation in  $(\alpha+\beta)$  Ti alloy under torsional fatigue.

## 5 CONCLUDING REMARKS

In the present work, crack initiation in biaxial fatigue was first modeled as the slip band formation in an individual grain constituting a polycrystalline metal. In modeled grains, normal directions of slip planes and slip directions on respective planes were independently given at random. It was assumed that the stress state in individual grain had variance from the stress state, to which the bulk material was subjected. Under this assumption, the stresses were also randomly assigned to each grain. As a crack initiation criterion, a slip-band crack was presumed to be initiated along the given slip direction on the specified slip plane when the resolved shear stress calculated in the slip direction exceeded a critical shear stress. The crack initiation life was evaluated using a dislocation pile-up model, in which the calculated resolved shear stress was incorporated. Simulations on crack initiation were carried out for three values of biaxiality; i.e. axial, torsional and combined axial-torsional modes. The relation between the distribution of crack orientations and the number of cycles for initiated cracks was able to be obtained by simulation using the proposed model. Simulated directions of initiated cracks under biaxial modes were compared with experimental results which had been observed in fatigue tests under axial, torsional and combined axial-torsional loading modes. As a whole trend, the estimation based on the proposed model showed a good agreement with the experimental observation.

## References

- [1] Hua, C. T., and Socie, D. F., Fatigue Damage in 1045 Steel under Variable Amplitude Biaxial Loading, *Fatigue Fract. Engng Mater. Struct.*, Vol. 8, pp. 101-114 (1985).
- [2] Bannatine, J. A., and Socie, D. F., Observation of Cracking Behavior in Tension and Torsion Low Cycle Fatigue, *ASTM STP 942*, pp. 899-921 (1988).
- [3] Hoshide, T., and Kusuura, K., Life Prediction by Simulation of Crack Growth in Notched Components with Different Microstructures and Under Multiaxial Fatigue, *Fatigue Fract. Engng Mater. Struct.*, Vol. 21, pp. 201-213 (1998).
- [4] Boettner, R. C., Laird, C., and McEvily, A. J., Jr., Crack Nucleation and Growth in High Strain-Low Cycle Fatigue, *Trans. AIME*, Vol. 233, pp. 379-387 (1965).
- [5] Laird, C., and Duquette, D. J., Mechanisms of Fatigue Crack Nucleation, *Corrosion Fatigue, NACE-2*, pp. 88-117 (1972).
- [6] Brown, M. W., and Miller, K. J., Initiation and Growth of Cracks in Biaxial Fatigue, *Fatigue Fract. Engng Mater. Struct.*, Vol. 1, pp. 231-246 (1979).
- [7] Tanaka, K., and Mori, T., A Dislocation Model for Fatigue Crack Initiation, *Trans. ASME, J. Appl. Mech.*, Vol. 48, pp. 97-103 (1981).
- [8] Inoue, T., Hoshide, T., Yoshikawa, T., and Kimura, Y., Slip-Band Behavior and Crack Initiation in Polycrystalline Copper under Multiaxial Low-Cycle Fatigue – A Damage Mechanics Approach, *Engng Fract. Mech.*, Vol. 25, No. 5/6, pp. 665-675 (1986).
- [9] Hoshide, T., Kakiuchi, E., and Hirota, T., *Fatigue Fract. Engng Mater. Struct.*, Vol. 20, No. 6, pp. 941-950 (1997).